Journal of Alloys and Compounds 509 (2011) 2031–2038

Contents lists available at ScienceDirect

Journal of Alloys and Compounds

journal homepage: www.elsevier.com/locate/jallcom

Microstructural changes of Guinier–Preston zones in an Mg–1.5 at% Gd–1 at% Zn alloy studied by HAADF-STEM technique

Kaichi Saito [a,*], Akira Yasuhara [b], Kenji Hiraga [c]

[a] Department of Materials Science and Engineering, Akita University, Akita 010-8502, Japan
[b] EM Application Group, EM Business Unit, JEOL Ltd., Tokyo 196-8558, Japan
[c] Institute for Materials Research, Tohoku University, Sendai 980-8577, Japan

ARTICLE INFO

Article history:
Received 8 July 2010
Received in revised form 20 October 2010
Accepted 22 October 2010
Available online 4 November 2010

Keywords:
Metals and alloys
Precipitation
Crystal structure
Microstructure
TEM

ABSTRACT

The microstructures of Guinier–Preston zones (GP-zones) precipitated in $Mg_{97.5}Gd_{1.5}Zn_1$ alloys annealed at 200 °C for various lengths of time have been thoroughly investigated by high-angle annular detector dark-field scanning transmission electron microscopy (HAADF-STEM) in combination with energy dispersive X-ray spectroscopy (EDS). The HAADF-STEM technique, which is capable of providing an atomic-scale *Z*-contrast image associated with heavier constituent elements in the alloys, has successfully allowed us to determine the atomic arrangement of Gd/Zn in the GP-zones. It is further evidenced that the GP-zones in the alloy have fairly variable microstructures with an advance of aging in the following way: wavy GP-zones → planar GP-zones → band-shaped (multi-layer) GP-zones (→ stacking faults).

1. Introduction

As the microstructural change occurring at the early stage of age-hardening of alloys, Guinier–Preston (GP) zone is one of the most profound effects. Experimentally, the precipitation of GP-zones was initially found by X-ray Laue diffraction measurements in Al–Cu alloys, and Guinier and Preston first detected the characteristic Cu segregation associated with GP-zone in the face-centred cubic Al-matrix [1,2]. The extension of GP-zones is generally too fine in scale to be resolved by early microscopy techniques. Not until recent years, did such improved microscopy techniques as high-resolution transmission electron microscopy (HRTEM) as well as high-angle annular detector dark-field scanning transmission electron microscopy (HAADF-STEM) enable us to confirm and identify the exact geometric features of GP-zones formed in an Al–Cu alloy [3]. More recently, those microscopy techniques have increasingly become utilized to explore characteristic microstructures of precipitates including GP-zones formed in various age-hardened Mg alloys having a hexagonal close packed (HCP) matrix [4–17].

An Mg–Gd alloy is one of the most prospective types of new structural materials capable of high strength properties combined with quite low density. In particular, Zn-doped Mg–Gd alloys have been found to be able to show considerable age-hardening effects, resulting from the formation of various types of precipitates such as β′-, β_1-, LPSO-phase and planar GP-zones [13–17]. In the most recent work that we made on Mg–Gd–Zn alloys with different compositions, it has become convincing that the microstructures of precipitates involving GP-zones could vary significantly depending on both, the atomic ratio of Gd/Zn in the alloy composition and the thermal history [17]. It was, indeed, indicated that the GP-zones become stabilized when the atomic ratio of Gd/Zn ranges between 1 and 1.5 and that they show a rather complex texture varied with an advance of aging. In order to elucidate such variable nature of the GP-zones, we have made further investigations of the GP-zones present in an $Mg_{97.5}Gd_{1.5}Zn_1$ alloy by making full use of HAADF-STEM technique in combination with EDS system equipped with a sub-nanometer probe.

2. Experimental procedures

An alloy with a nominal composition of $Mg_{97.5}Gd_{1.5}Zn_1$, which is characterized by the atomic ratio of Gd/Zn = 1.5, was prepared by melting Mg (99.9%), Gd (99.9%) and Zn (99.95%) metals by induction heating under an Ar gas in a carbon crucible. The alloy was homogenized at 520 °C for 2 h and then quenched immediately in water. Subsequently, the quenched alloy was divided into several parts, and the parts were subjected to aging treatments at 200 °C for various lengths of time. Specimens for transmission electron microscopy were cut from the aged samples and thinned by mechanical polishing, and finally completed by ion-milling. A transmission electron microscope, JEM-2100F (200 kV), was mainly used for making HAADF-STEM images. In addition, EDS analysis using a sub-nanometer probe was performed with the JEM-2100F microscope instrument operated at 200 kV.

* Corresponding author. Tel.: +81 18 889 2409; fax: +81 18 889 2409.
E-mail address: ksaito@ipc.akita-u.ac.jp (K. Saito).

0925-8388/$ – see front matter © 2010 Elsevier B.V. All rights reserved.
doi:10.1016/j.jallcom.2010.10.129

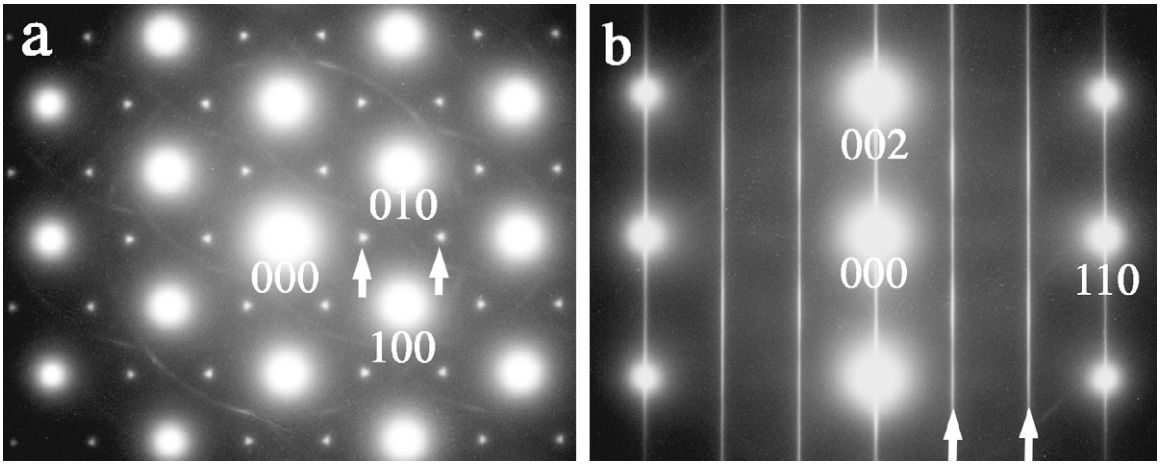

Fig. 1. Electron diffraction patterns of the $Mg_{97.5}Gd_{1.5}Zn_1$ alloy annealed at 200 °C for 100 h, taken with the incident beam parallel to the [0 0 1] (a) and [1 $\bar{1}$ 0] (b) directions of the HCP Mg-matrix. In both figures, arrows indicate the reflections originated from GP-zones.

3. Results and discussion

3.1. Stabilization of the GP-zones and their atomic structure

Fig. 1 shows electron diffraction patterns of the $Mg_{97.5}Gd_{1.5}Zn_1$ alloy annealed at 200 °C for 100 h, taken with the incident beam parallel to the [0 0 1] (a) and [1 $\bar{1}$ 0] (b) directions of the HCP Mg-matrix. In the patterns, there appear extra spots at 1/3 1/3 0-type positions indicated by arrows in Fig. 1(a) and streak reflections crossing at the same positions in Fig. 1(b), and these reflections both are originated from the planar GP-zones concerned. According to the previous work [16], it was found that an $Mg_{97}Gd_2Zn_1$ alloy with Gd/Zn = 2 undergoing a similar heat treatment has other weak spots due to the β' precipitates in the corresponding diffraction patterns. By contrast, the present alloy characterized by Gd/Zn = 1.5 allows the GP-zones only to become precipitated at this aging stage. It has been confirmed by our separate experiments that similar diffraction patterns to Fig. 1(a) and (b) also appear in $Mg_{98}Gd_1Zn_1$ and $Mg_{99}Gd_{0.5}Zn_{0.5}$ alloys with Gd/Zn = 1 annealed at 200 °C for 100 h [17]. It has, thus, been suggested that the atomic ratio of Gd/Zn is one of the key parameters aiming to control the microstructure of an age-hardened Mg–Gd–Zn alloy.

Fig. 2 shows an HAADF-STEM image of the $Mg_{97.5}Gd_{1.5}Zn_1$ alloy annealed at 200 °C for 100 h, taken with the incident beam perpendicular to the *c*-axis of the HCP Mg-matrix. Sharp line contrasts perpendicular to the *c*-axis in the image correspond to the planar GP-zones being parallel to close-packed planes of the Mg-matrix. Most of the GP-zones appearing at this aging stage show rather isolated and independent distribution with extensions ranging between 30 and 60 nm. Only occasionally, some parts of the GP-zones are closely aligned in pairs, taking the form of double GP-zones (see the areas marked by paired arrows in Fig. 2). It has, in fact, turned out that the double GP-zones in this alloy have a unique tendency to take such alignment with an interval of about 1.5 nm = 3*c*, where *c* is a lattice constant of the HCP Mg structure. This will be later discussed again with Fig. 11.

Fig. 3 shows results of elemental mapping analysis obtained from an area containing GP-zones by making use of a combined technique of HAADF-STEM and EDS. In Fig. 3(a), there are some GP-zones recognized as bright linear contrasts running vertically, two of which are indicated by arrows. The corresponding EDS mapping images related to Mg, Zn, and Gd are presented in Fig. 3(b)–(d), respectively, in which the locations of the GP-zones concerned are similarly indicated by arrows. The mapping images evidently show that heavier elements such as Zn and Gd are enriched and the light element of Mg is depleted on the locations of the GP-zones. In addition, quantitative chemical analyses making use of a sub-nanometer probe were made for five local areas around one individual GP-zone, as is shown by Fig. 4. The results are summarized in Table 1. The positions of 10 and 12 in Fig. 4, which are distanced furthest from the GP-zone, are found to be identified as areas consisting of α-Mg with slight solute of Gd, whereas the positions 13 and 14 being near to the GP-zone are those with the solute enrichment of Gd and Zn. These results indicate the tendency for solute atoms of Zn and Gd to migrate to the GP-zone which is formed by the segregation of considerable amounts of Zn and Gd. The EDS analysis of the GP-zone (Position 11) shows approximately the same contents of Gd and Zn, although the content of

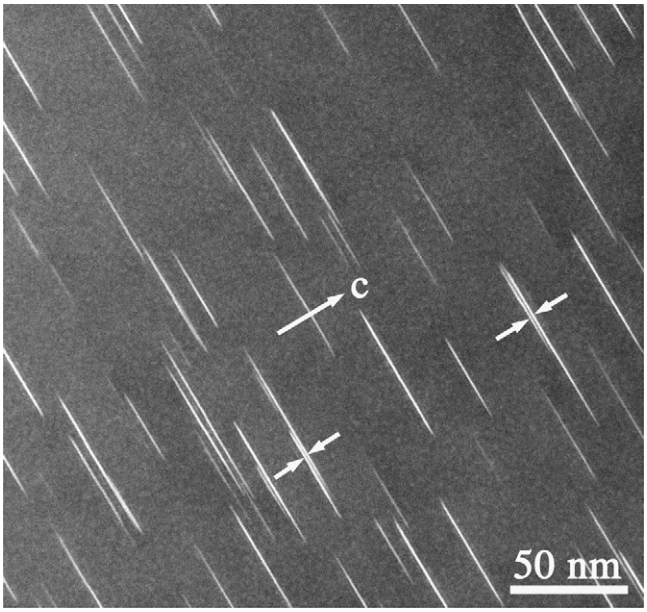

Fig. 2. HAADF-STEM image of the $Mg_{97.5}Gd_{1.5}Zn_1$ alloy annealed at 200 °C for 100 h, taken with the incident beam perpendicular to the *c*-axis of the HCP Mg-matrix. Sharp line contrasts correspond to planar GP-zones and in particular those indicated by paired arrows indicate double GP-zones with a definite interval.

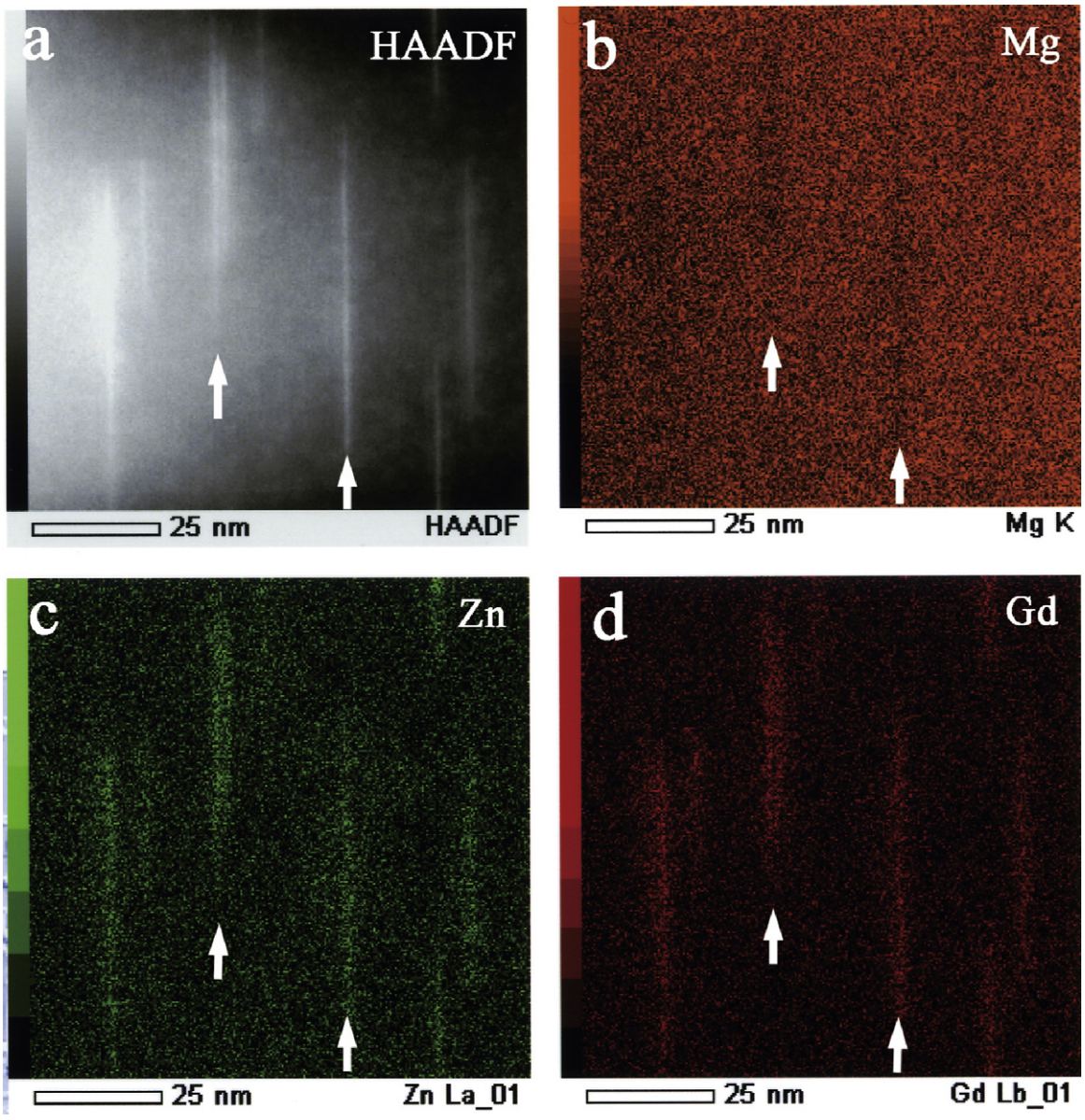

Fig. 3. HAADF-STEM image obtained from the $Mg_{97.5}Gd_{1.5}Zn_1$ alloy annealed at 200 °C for 100 h (a) and the corresponding EDS mapping images related to Mg (b), Zn (c) and Gd (d). Arrows in each figure indicate two of the identical GP-zones precipitated along the close-packed plane of the HCP Mg-matrix.

Mg obtained in this experiment is untrustworthy. This fact corroborates our previous result that the GP-zones in Mg–Gd–Zn alloys become stabilized when the atomic ratio of Gd/Zn ranges between 1 and 1.5.

Fig. 5 shows atomic-scale HAADF-STEM images of the GP-zones precipitated in the $Mg_{97.5}Gd_{1.5}Zn_1$ alloy annealed at 200 °C for 100 h, taken with two different viewing directions: the incident beam parallel to the [1 0 0] direction (a), and the [1 $\bar{1}$ 0] direction (b) of the HCP Mg-matrix. In both figures, dumbbell-like contrasts consisting of bright dots, each pair of which is distanced apart vertically by about 0.5 nm, are arranged horizontally with a constant interval of either about 0.3 nm for Fig. 5(a) or 0.5 nm for Fig. 5(b) along the GP-zones. These bright dots are supposed to represent such heavier atoms as Gd and/or Zn projected along the corresponding viewing directions, whereas weak bright dots recognized only in Fig. 5(a) represent Mg atoms in the matrix. Nishijima et al. [16] have proposed that the GP-zone formed in the $Mg_{97}Gd_2Zn_1$ alloy has such an ordered structure as indicated in Fig. 6(a) and (b), which illustrate three-dimensional arrangement and two-dimensional arrangement on the Gd/Zn-enriched planes, respectively. Atomic arrangements projected along the [1 0 0] and [1 $\bar{1}$ 0] are shown in Fig. 6(c) and (d), respectively. Fig. 6(c) and (d) shows that pairs of Gd/Zn atoms distanced apart by *c* are periodically arranged hori-

Table 1
Results of quantitative chemical analysis by EDS made for five local areas shown in Fig. 4.

Position no.	Mg	Zn	Gd
10	99.2	0	0.8
11	92	3.8	4.1
12	99.4	0	0.6
13	97.7	0.5	1.8
14	97.8	0.6	1.6

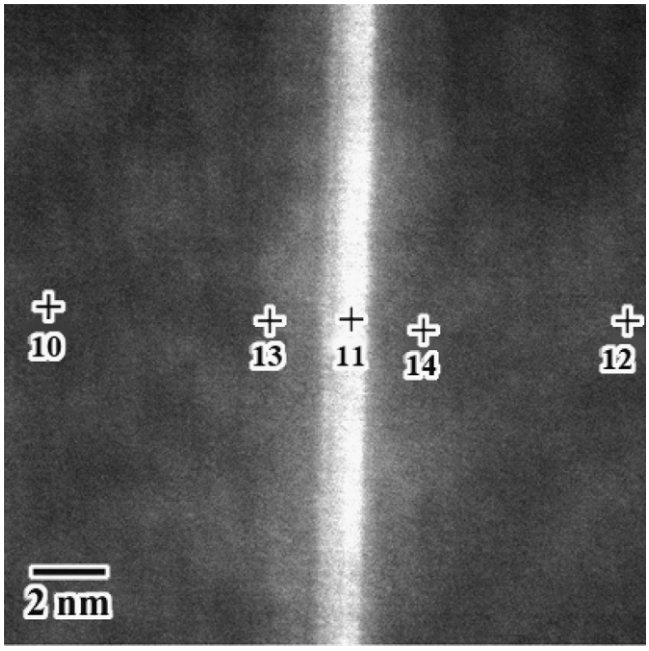

Fig. 4. HAADF-STEM image of the surrounding region of a GP-zone. Cross symbols with number letters indicate the local areas targeted for nano-probe EDS analysis. The results of the quantitative chemical analysis are summarized in Table 1.

zontally with an interval of either $d_{0\,1\,0} = \sqrt{3a/2} = 0.28$ nm for the [1 0 0] view or $3d_{1\,1\,0} = 3a/2 = 0.48$ nm for the [1 $\bar{1}$ 0] view, where a and c are lattice parameters of the HCP Mg structure. Such geometrical features can be clearly confirmed by Fig. 5. It is not at all strange that the less bright-dot-contrasts representing Mg atoms do not appear in the [1 $\bar{1}$ 0] view (Fig. 5(b)), as opposed to the case in the [1 0 0] view (Fig. 5(a)). This is simply due to the fact that the [1 1 0] inter-lattice distance ($d_{1\,1\,0} = a/2 = 0.16$ nm) of the HCP Mg-matrix is too short to be resolved by the instrument used in the present study. More interestingly, there is another remarkable feature associated with the GP-zones in Fig. 5(b): two parallel sets of the GP-zones marked by arrows have periodic arrangements of bright dots running horizontally with the same intervals but with definitely different phases from each other. The upper set of GP-zone is, indeed, laterally displaced relative to the lower set along the horizontal direction by a small distance, which may be approximately equal to $d_{1\,1\,0} = a/2 = 0.16$ nm. This will be discussed below in more detail with Fig. 11.

3.2. Variations of the GP-zones

Fig. 7 shows [1 $\bar{1}$ 0] diffraction patterns typically observed in the $Mg_{97.5}Gd_{1.5}Zn_1$ alloys of different aging stages, i.e. 200 °C for 20 h (a) and 200 °C for 200 h (b). Both patterns reveal diffuse streaks originated from the GP-zones crossing at 1/3 1/3 0-typed positions, as addressed in Fig. 1. Careful inspection allows us to notice that the streaks present in Fig. 7(a) show a rather wavy character, and that those in Fig. 7(b), by contrast, have discrete contrasts with intensity maximum located at the positions indicated by arrows. Besides, the maximum intensities recognized in Fig. 7(b) are found to have an approximate interval of one-sixth of the distance between 000 and 002 basic reflections. The presence of the discrete streaks leads us to deduce that there exist certain geometrical correlations between individual planar GP-zones, especially developing along their normal direction. Fig. 8 is an HAADF-STEM image of the $Mg_{97.5}Gd_{1.5}Zn_1$ alloy annealed at 200 °C for 20 h, taken with the incident beam parallel to the [1 $\bar{1}$ 0] direction of the HCP Mg-matrix. In this image, a number of GP-zones can be recognized as bright linear contrasts, having extensions of less than 30 nm. Each of the GP-zones appearing at this aging stage takes the form of an wavy-line, which can be understood to result in the wavy diffraction in Fig. 7(b). Fig. 9 is an atomic-scale [1 $\bar{1}$ 0] HAADF-STEM image targeting a few of the wavy GP-zones described above. Evidently, many of the GP-zones appearing at this aging stage are not completely planar enough

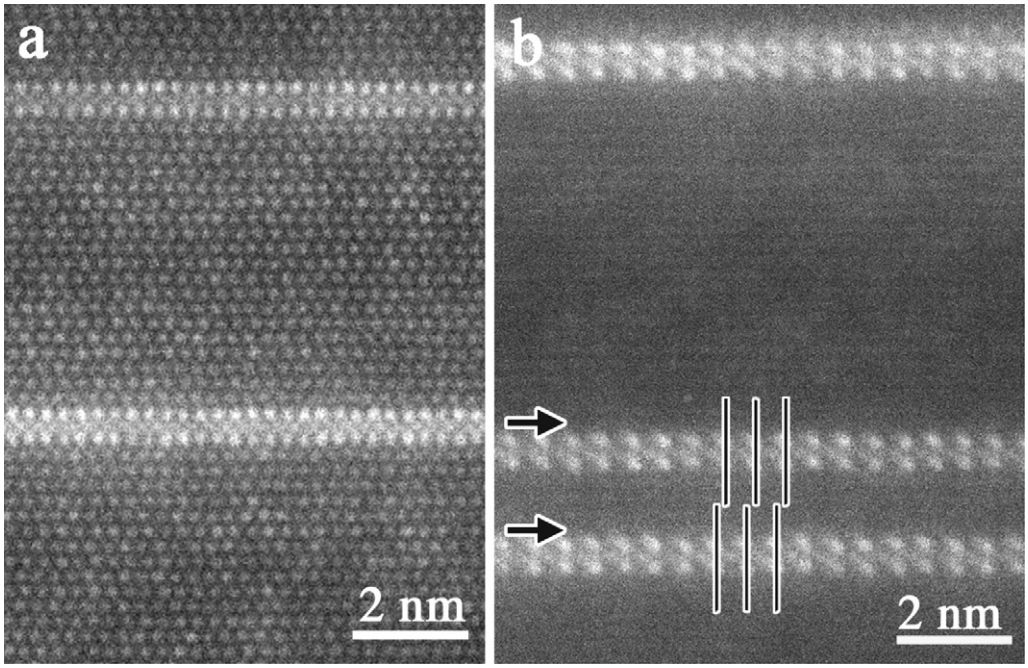

Fig. 5. Atomic-scale HAADF-STEM images of the GP-zones in the $Mg_{97.5}Gd_{1.5}Zn_1$ alloy annealed at 200 °C for 100 h, taken with the incident beam parallel to the [1 0 0] direction (a) and the [1 $\bar{1}$ 0] direction (b) of the HCP Mg-matrix. Brighter dots in both images correspond to Gd/Zn atoms in the GP-zones. Compare them with Fig. 6(c) and (d).

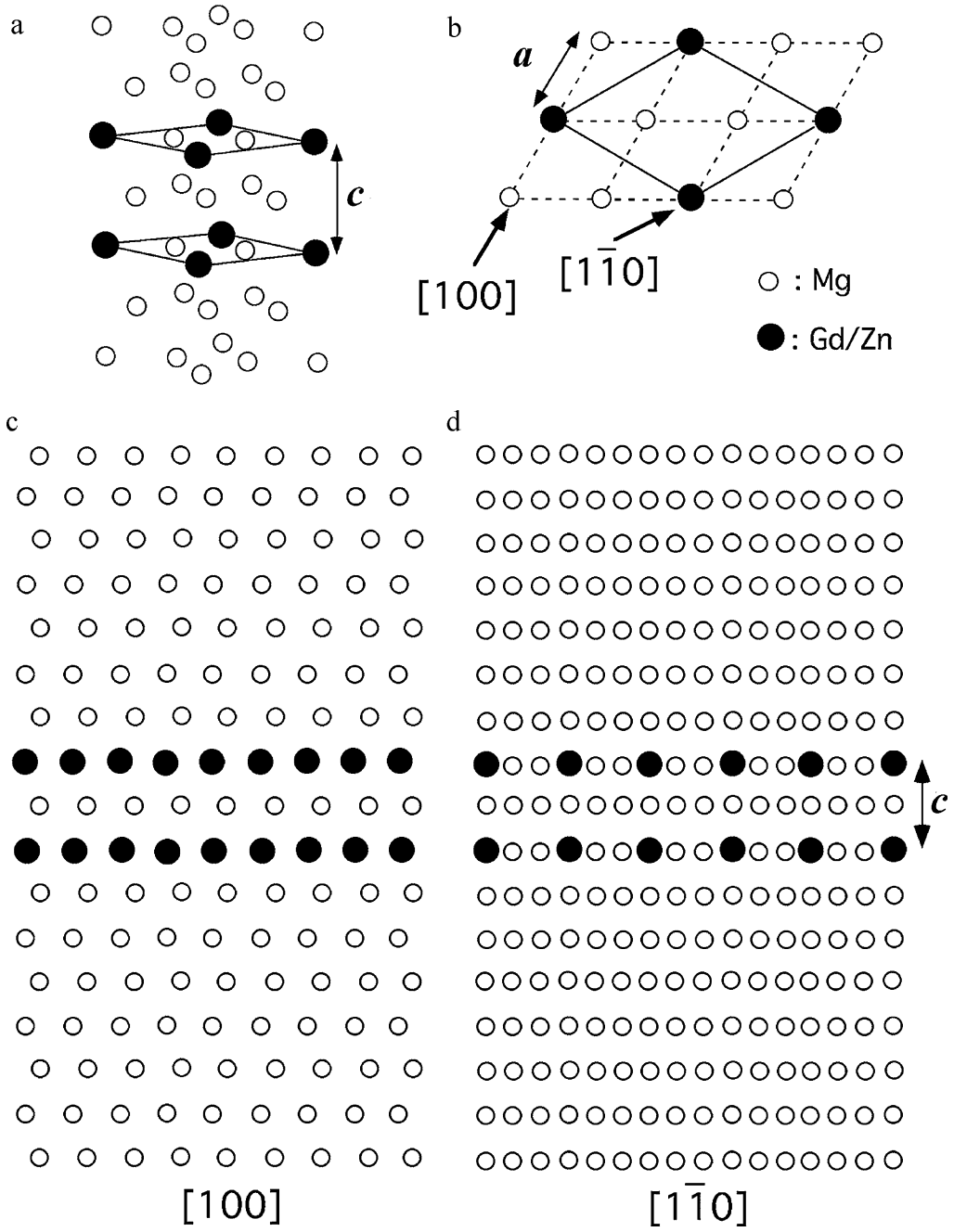

Fig. 6. Schematic drawings of the structure model of the GP-zone (a and b) and projected atomic arrangements along [1 0 0] (c) and [1 $\bar{1}$ 0] direction (d).

to keep running along the close-packed plane of the Mg matrix, but they are rather discontinued by accompanying small steps (for instance, see the areas marked by single arrows). There are also some GP-zones which appear in a thicker band, as represented by paired arrows. The appearance of thick bands is considered to be caused by the projection of GP-zones with some steps along the incident beam direction. The wavy character of GP-zones recognized in the image at intermediate magnification in Fig. 8 is, thus, attributed to incompletely planar GP-zones which are accompanied by small steps.

Fig. 10 is an HAADF-STEM image of the $Mg_{97.5}Gd_{1.5}Zn_1$ alloy annealed at 200 °C for 200 h, taken with the incident beam perpendicular to the *c*-axis of the HCP Mg-matrix. In the image, two distinct types of planar precipitates can be recognized: one is a type of precipitates with shorter extensions than approximately 40 nm running along the close-packed plane of the HCP Mg-matrix, and the other type is those with much longer extensions across the view. The shorter precipitates have been identified as GP-zones and the longer ones are stacking faults. Remarkably, many of the planar GP-zones are found to take the form of a band consisting of sequential stacks of 2–5 individual GP-zones apparently with definite intervals. Fig. 11 is an atomic-scale [1 $\bar{1}$ 0] HAADF-STEM image showing sequential stacks of GP-zones constituting a band, in which intervals of their stacks are mostly found to be 3*c* and sometimes 7*c*/2. It is natural to interpret that the sequential stacking of planar GP-zones along the normal direction produces discrete

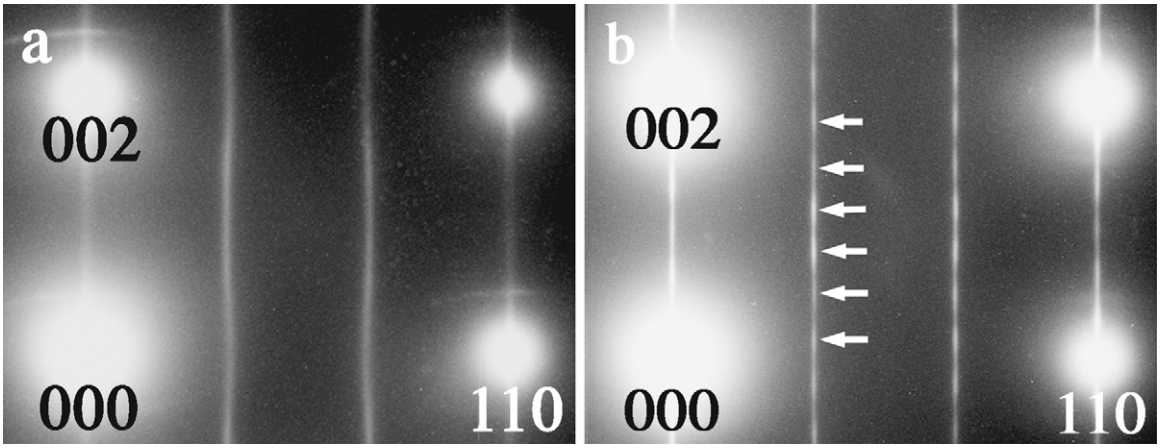

Fig. 7. Electron diffraction patterns typically found in the $Mg_{97.5}Gd_{1.5}Zn_1$ alloys of different aging stages, i.e. 200 °C for 20 h (a) and 200 °C for 200 h (b). Both patterns reveal the diffuse streaks originated from the GP-zones. Arrows in (b) indicate the locations of maximum intensities recognized along the diffuse streak.

streaks with intensity maximums in Fig. 7(b). It should be emphasized here again that one set of planar GP-zone is laterally displaced relative to the adjoining sets involving a certain phase shift, as was earlier addressed with Fig. 5(b). The phase shift of adjoining planar GP-zones allows us to assume three simple structure models based on the periodic stacking of GP-zones, as shown in Fig. 12, in which atomic arrangements projected along the [1 $\bar{1}$ 0] direction and illustrated diffraction patterns are shown. Probably, there coexist many uniquely grouped GP-zones in this alloy consisting of three sequential stacks of GP-zone, which are assumed to be caused by weak correlation between second nearest neighbour GP-zones. Under this interpretation, maximum intensities at the position of 1/3 1/3 2*n*/12 (*n* is integer) along the diffuse streaks in Fig. 7(b) can be reasonably understood by the mixture of the diffraction patterns in Fig. 12. After the classical nomenclature of GP-zone generally accepted for Al–Cu alloys [1,2], the planar GP-zones appearing in the Mg–Gd–Zn alloy annealed at 200 °C for 100 h, which are characterized by an isolated and independent distribution, may be classified as GP-I, and the band-shaped ones observed in the alloys annealed for 200 h are GP-II.

The stacking faults observed in Fig. 10 are considered to be thermo-dynamically stable precipitates, forming to replace the GP-zones after a substantial aging effect. In fact, it was indicated by separate experiments that the $Mg_{97.5}Gd_{1.5}Zn_1$ alloy allows the stacking faults only to become precipitated when annealed at such a higher temperature as 250 °C for 50 h. The stacking faults are formed by the segregation of Gd/Zn atoms, and they generally exhibit linear bright contrasts with approximately homogeneous intensity in the HAADF-STEM image, especially when it is imaged in the viewing direction normal to the *c*-axis of the HCP Mg matrix. This is exemplified by the contrast feature indicated by SF in Fig. 11 [15]. Although we are not certain about the real nature, the GP-zones are supposed to have a strong correlation activated among Gd and/or Zn atoms when they are formed, so that they can take

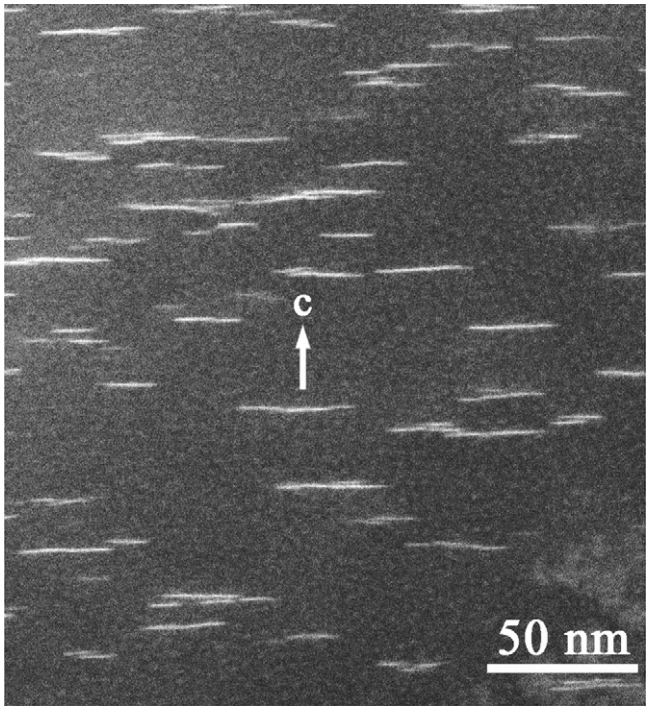

Fig. 8. HAADF-STEM image of the $Mg_{97.5}Gd_{1.5}Zn_1$ alloy annealed at 200 °C for 20 h, taken with the incident beam perpendicular to the *c*-axis of the HCP Mg-matrix. All of bright linear contrasts with extensions shorter than 30 nm correspond to the GP-zones. The GP-zones present at this aging stage exhibit wavy-lines.

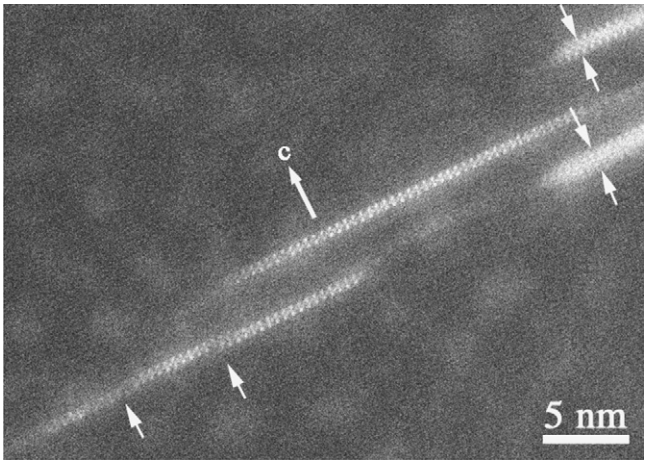

Fig. 9. Atomic-scale [1 $\bar{1}$ 0] HAADF-STEM image targeting a few of the wavy GP-zones, which was obtained from the $Mg_{97.5}Gd_{1.5}Zn_1$ alloys annealed at 200 °C for 20 h. Single arrows indicate the locations of the steps in the planar GP-zones, while paired arrows indicate the GP-zones with an increased thickness.

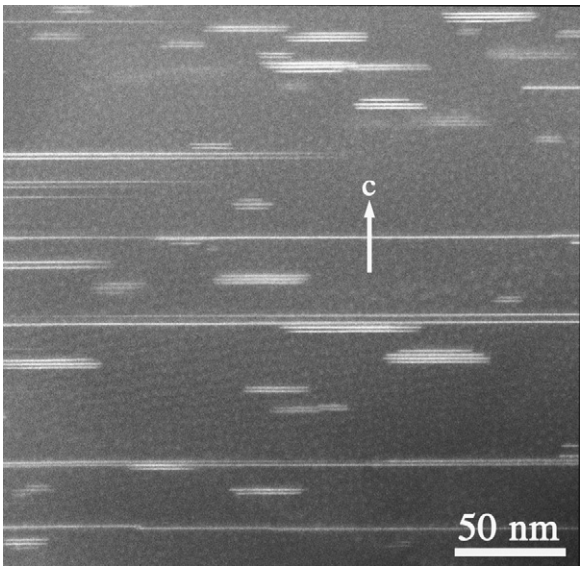

Fig. 10. HAADF-STEM image of the $Mg_{97.5}Gd_{1.5}Zn_1$ alloy annealed at 200 °C for 200 h, taken with the incident beam perpendicular to the *c*-axis of the HCP Mg-matrix. Band-shaped GP-zones formed by stacks of planar GP-zones as well as stacking faults with much longer extensions across the view are observed.

such ordered structures as discussed above. However, it seems that, with an advance of over-aging effect, the GP-zones gradually lose this correlation, and then become joined together with the neighbours reconstructing their structures, finally ending in the staking faults.

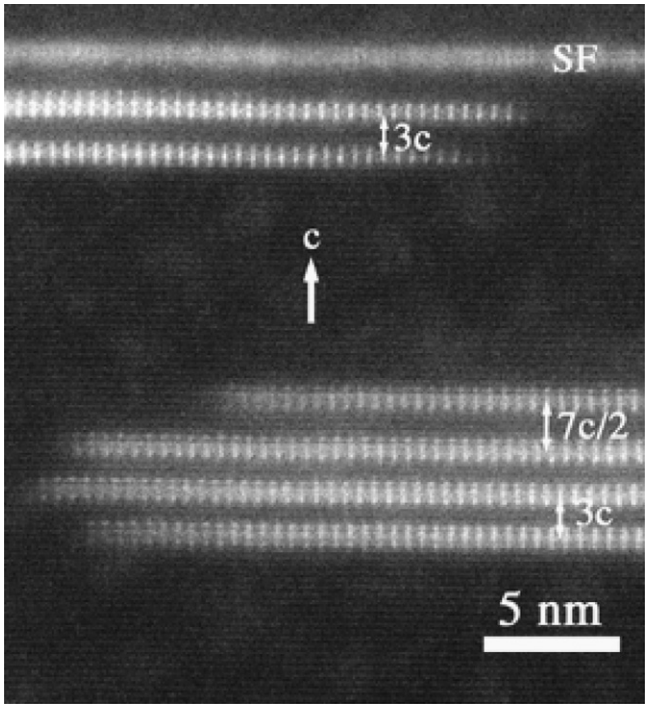

Fig. 11. Atomic-scale HAADF-STEM image of the $Mg_{97.5}Gd_{1.5}Zn_1$ alloy annealed at 200 °C for 200 h, taken with the incident beam perpendicular to the [1 $\bar{1}$ 0] direction of the HCP Mg-matrix. Note that stacks of GP-zones along the *c*-axis and phase shifts in periodical arrangements of dumbbell-like contrasts in adjoining planar GP-zones. SF indicates a stacking fault.

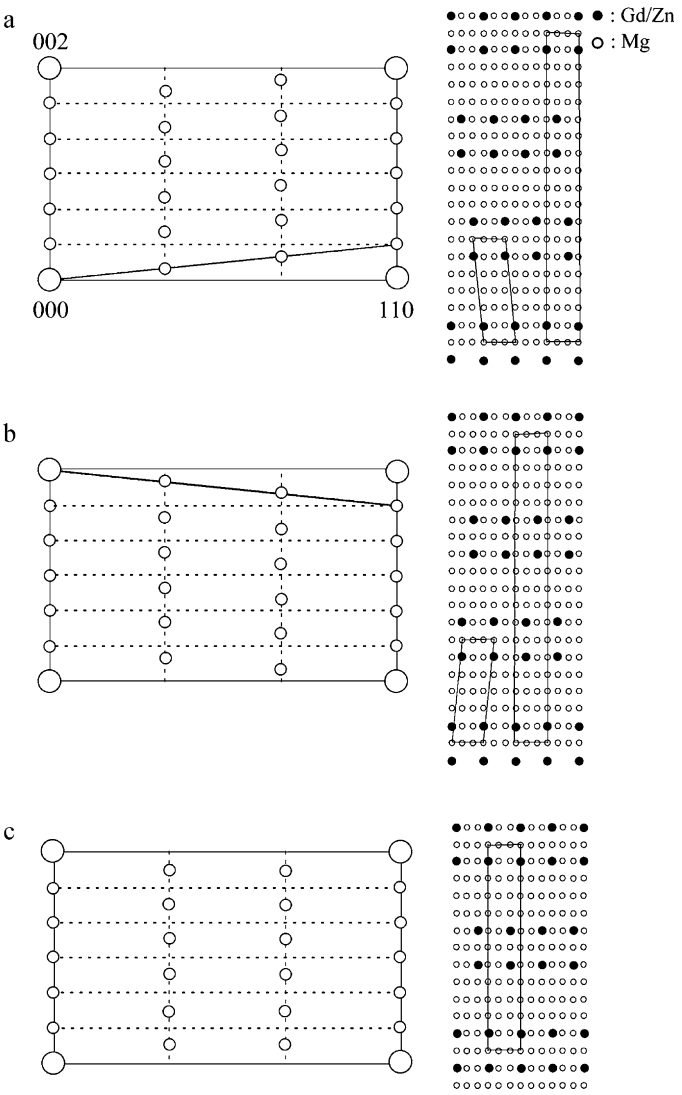

Fig. 12. Three structure models formed by periodic stacks of the GP-zones, illustrated in the [1 $\bar{1}$ 0] projection (the right side), and corresponding diffraction patterns (the left side).

4. Conclusions

The microstructures of GP-zones formed in $Mg_{97.5}Gd_{1.5}Zn_1$ alloys annealed at 200 °C for various lengths of time have been investigated by means of HAADF-STEM in combination with EDS. The EDS analysis has made us convinced that the doping of approximately equal amounts of Gd and Zn in this Mg alloy is essential for the stability of the GP-zone. The HAADF-STEM observations have also revealed that there is a fairly variable nature in microstructures of the GP-zones with an advance of aging, demonstrating that the aging behaviour associated with the GP-zones is as follows: wavy GP-zones → planar GP-zones → band-shaped (multi-layer) GP-zones (→ stacking faults). In the course of aging, each of the individual GP-zones increasingly shows a marked tendency to have a certain correlation with the neighbouring GP-zones. The solute enrichment of Gd and Zn at the matrix near GP-zones, which has been detected by EDS, is produced by the migration of Gd and Zn atoms to the GP-zones, and the solute enrichment is supposed to have a cause for the formation of the band-shaped GP-zones. Nonetheless, the GP-zones are metastable precipitates and are completely replaced by stacking faults by a substantial aging effect.

Acknowledgements

This work was partly supported by the Center for Integrated Nanotechnology Support at Tohoku University and also by "Nanotechnology Network Project" of the Ministry of Education, Culture, Sports, Science, and Technology (MEXT) of the Japanese Government.

References

[1] A. Guinier, Nature 142 (1938) 569.
[2] G.P. Preston, Nature 142 (1938) 570.
[3] T.J. Konno, K. Hiraga, M. Kawasaki, Scripta Mater. 44 (2001) 2303–2307.
[4] D.-H. Ping, K. Hono, J.F. Nie, Scripta Mater. 48 (2003) 1017–1022.
[5] J.C. Oh, T. Ohkubo, T. Mukai, K. Hono, Scripta Mater. 53 (2005) 675–679.
[6] X. Gao, S.M. Zhu, B.C. Muddle, J.F. Nie, Scripta Mater. 53 (2005) 1312–1326.
[7] X. Gao, J.F. Nie, Scripta Mater. 58 (2008) 619–622.
[8] M. Matsuura, K. Konno, M. Yoshida, M. Nishijima, K. Hiraga, Mater. Trans. 47 (2006) 1264–1267.
[9] M. Nishijima, K. Hiraga, T. Itoi, M. Hirohashi, Mater. Trans. 47 (2006) 805–810.
[10] M. Nishijima, K. Yubuta, K. Hiraga, Mater. Trans. 48 (2007) 84–87.
[11] M. Nishijima, K. Hiraga, M. Yamasaki, Y. Kawamura, Mater. Trans. 48 (2007) 476–480.
[12] M. Nishijima, K. Hiraga, M. Yamasaki, Y. Kawamura, Mater. Trans. 50 (2009) 1747–1752.
[13] M. Nishijima, K. Hiraga, M. Yamasaki, Y. Kawamura, Mater. Trans. 47 (2006) 2109–2112.
[14] M. Nishijima, K. Hiraga, Mater. Trans. 48 (2007) 10–15.
[15] M. Yamasaki, M. Sasaki, M. Nishijima, K. Hiraga, Y. Kawamura, Acta Mater. 55 (2007) 6778–6805.
[16] M. Nishijima, K. Hiraga, M. Yamasaki, Y. Kawamura, Mater. Trans. 49 (2008) 227–229.
[17] K. Saito, M. Nishijima, K. Hiraga, Mater. Trans. 51 (2010) 1712–1714.